

B physics at the $D\bar{O}$ Experiment at Fermilab

Vivek Jain

Department of Physics, State University of New York,
Albany, NY

Abstract

We discuss recent B physics results from the $D\bar{O}$ experiment at Fermilab¹. The results presented here use data sets with integrated luminosities ranging from $\sim 200 - 440 \text{ pb}^{-1}$, collected at the Tevatron, between April 2002 and August 2004, at a center of mass energy of $p\bar{p}$ collisions of 1.96 TeV.

PACS Nos.: 13.20.He, 13.25.Hw, 14.20.Mr, 14.40.Nd, 14.40.Gx

1 Introduction

An understanding of flavour dynamics is crucial since any unified theory will have to account for the presence of three left-handed families, measured mixing angles and masses of various quarks and hadrons, *etc.* The study of bottom hadrons provides unique insights into the nature of the weak as well as the strong interaction, and also provides a window into beyond-Standard Model (BSM) effects[1].

The study of bottom hadrons at the Fermilab Tevatron ($p\bar{p}$ collisions at a center of mass energy of 1.96 TeV) has many advantages over that at the currently operating e^+e^- “ B -factories” at SLAC and KEK, *viz.*, the production cross-section of $b\bar{b}$ quarks is about 150,000 times larger, and all species of bottom hadrons are produced.² However, experimental conditions are not as clean; for instance, the total $p\bar{p}$ cross-section is more than two orders of magnitude larger than that for $b\bar{b}$ production. This implies that experiments at the Tevatron are crucially dependent on designing appropriate triggers; the collision rate at $D\bar{O}$ is about 2.5 MHz, whereas the experiment can only write out data at about 50-100 Hz.

The B physics program at $D\bar{O}$ is designed to be complementary to the program at the B -factories at SLAC and KEK and includes studies of B_s oscillations, searches for rare decays such as $B_s \rightarrow \mu^+\mu^-$, B spectroscopy, *e.g.*, B_J^* , lifetimes of B hadrons, search for the lifetime difference in the B_s CP eigenstates, study of beauty baryons, B_c mesons, quarkonia (J/ψ , χ_c , Υ), b production cross-section, *etc.*

One of the more important topics in B physics is the search for $B_s\bar{B}_s$ mixing. Global fits, assuming that the CKM matrix is unitary and the Standard Model (SM) is correct, indicate that the 95% CL interval[2] for the mixing frequency, ΔM_s , is [14.2-28.1] ps^{-1} . The current limit³ is $\Delta M_s > 14.9\text{ps}^{-1}$ at the 95% CL[2]. A measured value of ΔM_s much larger than the upper limits given here could imply new physics contributing to the box diagrams, *e.g.*, extra Higgs bosons or squarks and/or gluinos[3].

¹Invited review article to appear in Modern Physics Letters A.

²Although all B -hadron species were also produced at LEP, $\sigma_{b\bar{b}}$ at the Tevatron is about 20,000 times larger.

³The limit is derived by combining limits from 13 different measurements.

2 DØ detector

For the current run of the Tevatron (Run II), the DØ detector went through a major upgrade[4]. The inner tracking system was completely revamped. The detector now includes a Silicon tracker, surrounded by a Scintillating Fiber tracker, both of which are immersed in a 2 Tesla solenoidal magnetic field. Pre-shower counters, to aid in electron and photon identification are located before the calorimeter. The muon system has also been improved, *e.g.* more shielding was added to reduce beam background. New trigger and data acquisition systems were also installed.

The DØ detector has excellent tracking and lepton acceptance. Tracks with pseudo-rapidity (η) as large as 2.5 ($\theta \sim 10^\circ$) and transverse momentum (p_T) as low as 180 MeV/c are reconstructed.

The muon system can identify muons within $|\eta| < 2.0$. The minimum p_T of the reconstructed muons varies as a function of η . In most of the results presented here, we required muons to have $p_T > 2$ GeV/c. Low p_T electron identification is being worked on, currently we are limited to $p_T > 2$ GeV/c and $|\eta| < 1.1$; however, we are working to improve both the momentum and η coverage.

DØ employs a three level trigger. Triggers at Level 1, which are formed by individual detector sub-systems, and Level 2, where they are further refined, are constructed using custom hardware. At Level 3, the entire event is read out by a farm of computers which perform a simplified event reconstruction to further refine the selection criteria for interesting events. Currently, the input rate to Level 1 is 2.5 MHz and the output is 1600 Hz; the output rates for Level 2 and 3 are 800 Hz and 60 Hz respectively. Improvements are foreseen that could improve the output rates to 2-2.5 kHz, 1.2 kHz and 100 Hz for Levels 1, 2 and 3, respectively.

3 Data Sample

The results presented here are based on data collected between April 2002 and August 2004. The data correspond to an integrated luminosity of about 440 pb⁻¹, however the analyses presented here used anywhere from 200-440 pb⁻¹. Events enriched in B hadrons were collected with a dimuon and single muon triggers. To reduce the data rate, a luminosity dependent prescale was applied to the single muon trigger (the prescale was 1 for instantaneous $\mathcal{L} < 20 \times 10^{30}$ cm⁻²s⁻¹). Both triggers require that muons have hits in all layers of the muon system which implies that they have total momentum ≥ 3 GeV.

Many of these results have been accepted for publication. Details on the other analyses can be found on the DØ B physics group web page[5].

4 New Particles

We first review results dealing with particles which either have never been seen before or have been recently observed, *viz.*, $X(3872)$, $B_J^*(5732)$ and B_c .

4.1 X(3872)

$X(3872)$ was first observed by the Belle collaboration[6] via $B \rightarrow X(3872)K$, $X \rightarrow J/\psi\pi^+\pi^-$, and was subsequently observed (inclusively) by the CDF collaboration[6] in $p\bar{p}$ collisions (in the same $X(3872)$ final state). In Fig. 1(a), we present evidence for $X(3872) \rightarrow J/\psi\pi^+\pi^-$, observed by the DØ collaboration[7]; the inset shows the mass distribution of $J/\psi \rightarrow \mu^+\mu^-$ candidates. To improve resolution, the mass difference $\Delta M = M(\mu^+\mu^-\pi^+\pi^-) - M(\mu^+\mu^-)$ is used. We observe

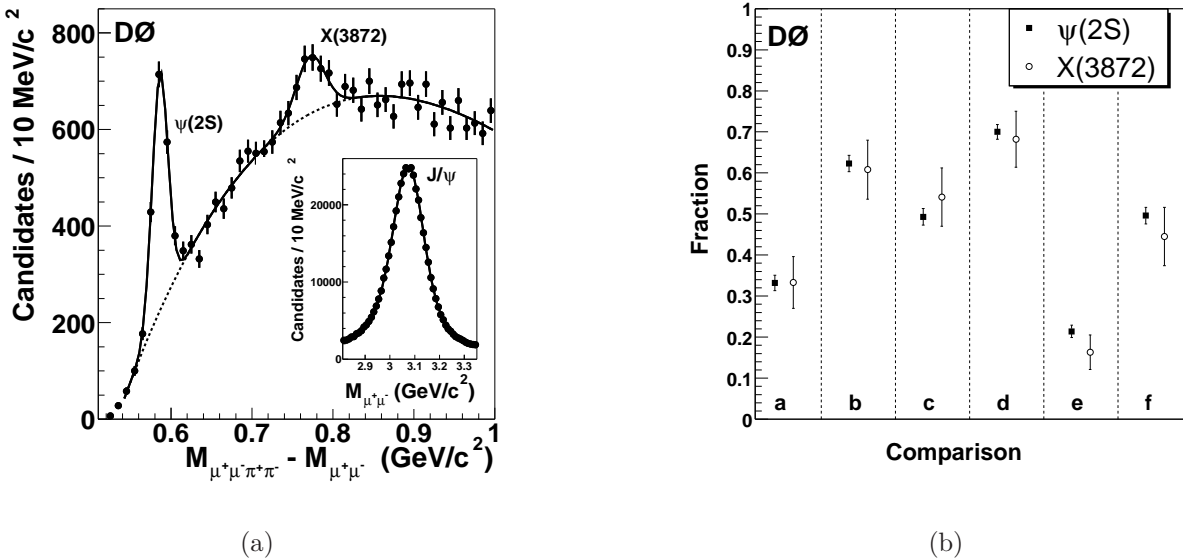


Figure 1: (a) $\Delta M = M(\mu^+\mu^-\pi^+\pi^-) - M(\mu^+\mu^-)$ after all cuts. In the inset, we show the $J/\psi \rightarrow \mu^+\mu^-$ mass spectrum. (b) Comparison of various production and decay variables for the X(3872) and $\psi(2S)$ - see text for details.

522 ± 100 X(3872) candidates and measure $\Delta M = 774.9 \pm 3.1(stat) \pm 3.0(syst)$ MeV/ c^2 ; this value is consistent with other measurements of $M(X(3872))$ and is based on an integrated luminosity of 230 pb^{-1} .

It is not known whether the X(3872) is a normal charmonium state or something more exotic, *e.g.*, $D\bar{D}$ molecule or ccg hybrid[8]. To understand its nature we compare some of its production and decay properties with the well-known charmonium state $\psi(2S)$ [9], which can also be seen in Fig 1(a). In Fig. 1(b), we present the fraction of X(3872) ($\psi(2S)$) candidates which satisfy certain criteria, (a) $p_T > 15$ GeV/ c , (b) rapidity, $|y| < 1$, (c) helicity of the $\pi\pi$ system, $|\cos(\theta_\pi)| < 0.4$, (d) effective proper decay length < 0.01 cm, (e) Isolation⁴ = 1 and (f) helicity of the $\mu\mu$ system, $|\cos(\theta_\mu)| < 0.4$. In all these variables, the X(3872) appears to behave like the $\psi(2S)$.

Other studies include searching for the charged partner, *e.g.*, $X^+ \rightarrow J/\psi\pi^+\pi^0$ or for radiative decays like $X(3872) \rightarrow \chi_c\gamma$; a signal for the former would rule out the charmonium hypothesis whereas a signal for the latter would confirm it as a charmonium state.

4.2 P-wave mesons: $B_J^*(5732)$

Hadrons which contain one heavy quark, $m_Q \gg \Lambda_{QCD}$, are subject to additional QCD symmetries. As $m_Q \rightarrow \infty$, the heavy quark decouples and the properties of the hadron are given by light degrees of freedom (*Ldof*), *i.e.*, light quark(s) and gluons; this is known as Heavy Quark Symmetry (HQS)[10]. In this limit, mesons belong to degenerate doublets given by $J^P = (j_l \pm 1/2)^{\pi_l}$, where J, j_l are the total angular momenta of the meson and the *Ldof*, and P, π_l are their respective parities; also, $j_l = s_l + L$, where s_l is the spin of the *Ldof* and L is the angular momentum between the *Ldof* and the heavy quark. Degeneracy is broken due to finite m_Q and so the effect is larger for charm mesons than bottom mesons.

$L = 0$ gives one doublet with $j_l = \frac{1}{2}$ and $J = 0, 1$ which corresponds to the well-measured

⁴Isolation is defined as the ratio of the p_T of the X(3872) to that of the X(3872) and all other particles within a cone of 0.7

B, B^* mesons[9]. For $L = 1$, we get two doublets denoted as $j_l = \frac{1}{2}, J = 0, 1$ and $j_l = \frac{3}{2}, J = 1, 2$; collectively, these four mesons are referred to as B_J^* mesons. Angular momentum and parity conservation constrains the strong decays of the $L = 1$ mesons, with the $J = 0$ state expected to decay to $B\pi$, $J = 1$ states to $B^*\pi$ and $J = 2$ state to $B\pi$ and $B^*\pi$; $j_l = \frac{1}{2}$ decay via S-wave and are expected to be broad while $j_l = \frac{3}{2}$ states decay via D-wave and are expected to be narrow.

In the case of (non-strange) charm mesons all four $L = 1$ states have been observed, and their behaviour agrees with expectations[9, 11]. On the other hand, the case of $L = 1$ charm-strange mesons states is more interesting. The $j_l = \frac{3}{2}$ doublet decays to the favoured $D^{(*)}K$ final states[9], whereas the $j_l = \frac{1}{2}$ states were lighter than expected and could only decay to $D_s^{(*)}\pi^0$ final states[12]; this also causes them to be narrower than expected[13].

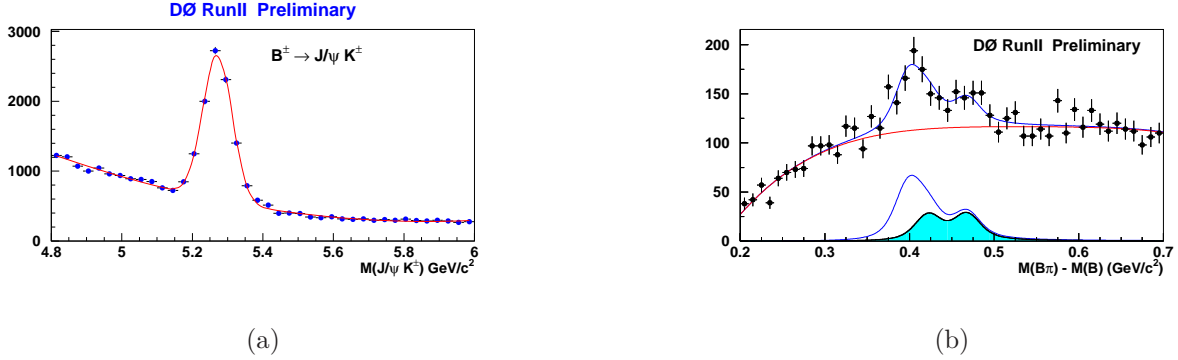


Figure 2: Mass distribution for (a) $B^+ \rightarrow J/\psi K^+$, (b) B^{**} presented as $\Delta M = M(B\pi) - M(B)$

In the case of B_J^* , an excess of events has been observed with an average mass of $5698 \pm 8 \text{ MeV}/c^2$, although the four $L = 1$ states have not been individually observed[9]; in addition, only one of the experiments exclusively reconstructed the B meson.

We use our large sample of fully reconstructed B mesons, (a) $B^+ \rightarrow J/\psi K^+$ (Fig 2(a)), (b) $B^0 \rightarrow J/\psi K^{*0}$ and (c) $B^0 \rightarrow J/\psi K_s^0$ to search for the narrow B_J^* mesons; in $\sim 350 \text{ pb}^{-1}$ of data, we have the following yields, (a) 7217 ± 127 , (b) 2826 ± 93 and (c) 624 ± 41 . Since the mass difference between B_J^{*+} and B_J^{*0} is expected to be small, we add all three B modes and perform a combined search. In addition, to reduce resolution effects, we plot the mass difference, $\Delta M = M(B^{+0}\pi^{\pm}) - M(B^{+0})$, where the π^{\pm} is required to be consistent with coming from the primary vertex.

The mass difference plot, as shown in Fig. 2(b) has a structure consistent with three components which correspond to the two states, B_1 and B_2^* (which make up the $j_l = \frac{3}{2}$ doublet), (a) $B_1 \rightarrow B^*\pi^{\pm}$, (b) $B_2^* \rightarrow B^*\pi^{\pm}$ and (c) $B_2^* \rightarrow B\pi^{\pm}$. The B^* decays to a $B\gamma$ final state and the soft photon (in the c.m. $E_\gamma \sim 46 \text{ MeV}$) is not observed. This causes ΔM from the (a) and (b) to be shifted down by 46 MeV while it is in the correct place for (c). Allowing for all three of these sources in the final fit, we observe a total of 536 ± 114 events. Using input from HQS, we assign 273 ± 59 to (a) and 131 ± 30 events each to (b) and (c). In addition, we measure $M(B_1) = 5724 \pm 4(\text{stat}) \pm 7(\text{syst}) \text{ MeV}/c^2$, $M(B_2^*) - M(B_1) = 23.6 \pm 7.7 \pm 3.9 \text{ MeV}/c^2$, and assuming that $\Gamma_2 = \Gamma_1$ we obtain $23 \pm 12 \pm 9 \text{ MeV}$ for the natural widths, in agreement with theoretical expectations[14]. This is the first observation of the narrow B_J^* states.

Future studies will include separate fits for B_J^{*+} and B_J^{*0} , measuring the production rate of $L = 1$ B mesons relative to $L = 0$ B mesons, measurement of the spin-parity of these states, and a search for B_{sJ}^* .

4.3 B_c meson

The B_c meson consisting of a b and a c quark is the heaviest of the flavoured ground state mesons that can exist; the top quark decays before it can hadronize into a meson. Since it consists of two heavy quarks, theoretical tools used to describe $c\bar{c}$ and $b\bar{b}$ mesons can be employed in its study[15]. The B_c meson has non-zero flavour and thus it only has weak decays. It has been observed by the CDF collaboration[16]; the yield was $20.4_{-5.5}^{+6.2}$ events in 110 pb^{-1} of $p\bar{p}$ collisions. The lifetime is expected to be closer to charm hadron lifetimes ($\leq 1 \text{ ps}$) than to those of other beauty hadrons ($\sim 1.5 \text{ ps}$).

A particularly attractive mode for its observation at DØ is the semileptonic decay, $B_c \rightarrow J/\psi\mu\nu X$; the presence of three muons in the final state makes it easy to trigger on. In addition, backgrounds (branching fraction) are expected to be lower (higher) than for the exclusive mode, $J/\psi\pi$. However, due to missing particles in the final state, *e.g.*, neutrino (and maybe pions), the determination of the mass and lifetime has to rely on Monte Carlo simulations based on the ISGW model[17]. Systematic effects are studied by using different decay models, *e.g.*, V-A, *etc.*

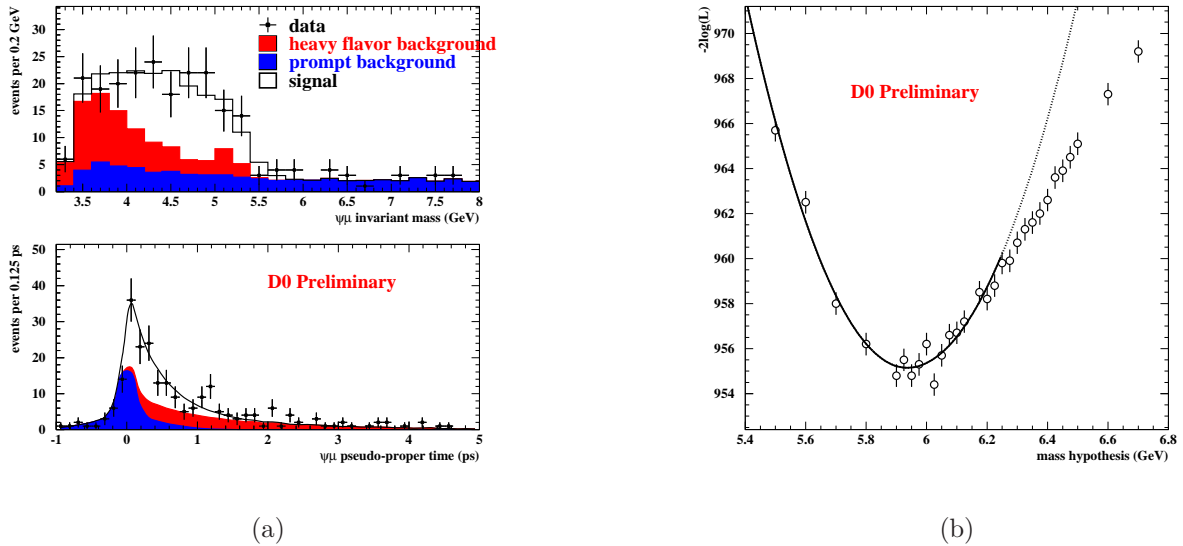


Figure 3: (a) The $J/\psi\mu$ invariant mass and pseudo-proper decay time distributions of the data candidates (points), with the results of the best combined mass and lifetime likelihood fit overlaid, (b) Distribution of $-2\log(\mathcal{L})$ returned by the combined fit at a variety of mass hypotheses.

We use $\sim 210 \text{ pb}^{-1}$ of data to study this particle[18]. We combine a J/ψ and a muon to form B_c candidates; a background sample consisting of a J/ψ and one track (which is not a muon) is also formed. The latter sample is used to study the heavy flavour background. Since there are missing particles in the final state, the momentum of the $J/\psi\mu$ system must be corrected to account for them. A simultaneous fit to the mass and pseudo-proper decay time⁵ of the J/ψ system is performed and the results are shown in Fig. 3(a). In Fig. 3(b), we show the distribution of $-2\log(\text{likelihood})$ from the combined fit at a variety of mass hypotheses. A clear minimum is observed at $5.95 \text{ GeV}/c^2$.

We observe $95 \pm 12 \pm 11$ B_c candidate events, and determine the mass and lifetime to be $5.95_{-0.13}^{+0.14} \pm 0.34 \text{ GeV}/c^2$ and $0.448_{-0.096}^{+0.123} \pm 0.121 \text{ ps}$, respectively, which agrees with the previous measurement and theoretical predictions[15, 16].

⁵This is converted to the true proper decay time by the application of a correction factor to account for missing particles.

5 Beyond Standard Model studies

Purely leptonic decays of the B meson, *e.g.*, $B_s \rightarrow \mu^+ \mu^-$, are examples of Flavour Changing Neutral Currents (FCNC). In the SM, such decays are forbidden at tree level and proceed through the higher order box diagrams, and consequently have very low rates. For instance, $\mathcal{B}(B_s \rightarrow \mu^+ \mu^-)$ is expected[19] to be $(3.42 \pm 0.54) \times 10^{-9}$, whereas the previous best experimental limit[20] is 5.8×10^{-7} at the 90% C.L.

Such modes are very interesting because in many BSM models, *e.g.* 2-Higgs Doublet, Super Symmetry, mSUGRA models, Grand Unified theories based on SO(10) *etc.*, the rate can be enhanced by as much as three orders of magnitude[21].

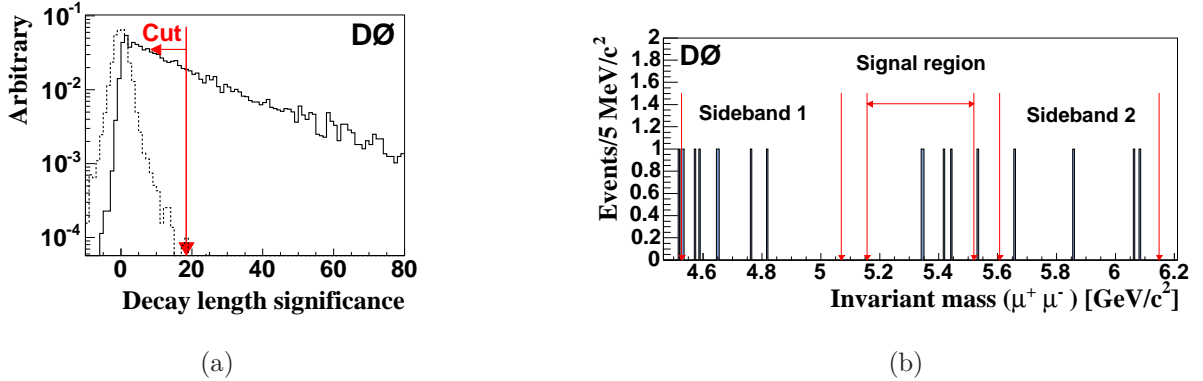


Figure 4: (a) $(L_{xy}/\sigma_{L_{xy}})$ after the preselection for signal MC (solid line) and data events (dashed line) from the sidebands. Arrow indicates the discriminating value that was obtained after optimization. Normalization is done on the number of signal MC and sideband data events after preselection, (b) Invariant mass of the remaining events of the full data sample after optimized requirements on the discriminating variables

We use 240 pb^{-1} of data to search for this decay mode[22]. After the initial (pre)selection criteria *e.g.* muon quality, vertex consistency, $pT(B_s)$, *etc.*, we use three additional variables to discriminate signal-like events from background, (a) Decay Length significance ($L_{xy}/\sigma_{L_{xy}}$) of the B_s vertex, (b) Isolation of the $\mu^+ \mu^-$ pair, and (c) Angle between the B_s momentum and decay vector. These three variables were optimized using a Monte Carlo for the signal and B_s mass sidebands in data for estimating the background. In Fig. 4(a), we show the results for one of these variables, the optimal cut value is $L_{xy}/\sigma_{L_{xy}} > 18.5$, as indicated by the arrow. After all (optimized) selection criteria, the prediction is that in the $(\pm 3\sigma)$ mass region around the B_s , there should be 3.7 ± 1.1 background events. With these selection criteria, we observe 4 events, as shown in Fig. 4(b).

To determine an upper limit, we use $B^+ \rightarrow J/\psi K^+$ as a normalizing mode; the relative fragmentation of the b quark into B^+ and B_s has to be taken into account. We set an upper limit, $\mathcal{B}(B_s \rightarrow \mu^+ \mu^-) < 4.1 \times 10^{-7}$ at the 90% C.L., which is currently the most stringent limit.

6 Lifetimes

An understanding of the pattern of lifetimes of heavy hadrons provides insight into non-perturbative QCD. In the last few years, theoretical tools using a rigorous approach based on the heavy quark expansion (in inverse powers of the heavy quark mass) have been developed[23]. Predictions for bottom hadrons are on a much firmer footing than for charm hadrons. Theoretical errors are further

reduced on predictions for ratios of lifetimes[24]; for instance, $\frac{\tau(B^+)}{\tau(B^0)} = 1.06 \pm 0.02$, $\frac{\tau(B_s)}{\tau(B^0)} = 1.00 \pm 0.01$, $\frac{\tau(\Lambda_b)}{\tau(B^0)} = 0.88 \pm 0.05$.

6.1 Measurement of $\frac{\tau(B^+)}{\tau(B^0)}$

Using a large sample of B semi-leptonic decays in 440 pb^{-1} of data, DØ has made a precision measurement of $\frac{\tau(B^+)}{\tau(B^0)}$ [25]. B mesons were detected via the $B \rightarrow \mu^+ \nu \bar{D}^0 X$ mode (which had 126073 ± 610 events), and categorized as the “ D^{*-} ” or the “ \bar{D}^0 ” sample; the former contains identified $D^{*-} \rightarrow \bar{D}^0 \pi^-$ events and is dominated by B^0 candidates while the latter contains the remaining events and is dominated by B^+ events. The ratio of events in the two samples as a function of proper time is primarily a function of the lifetime difference between the B^+ and the B^0 .

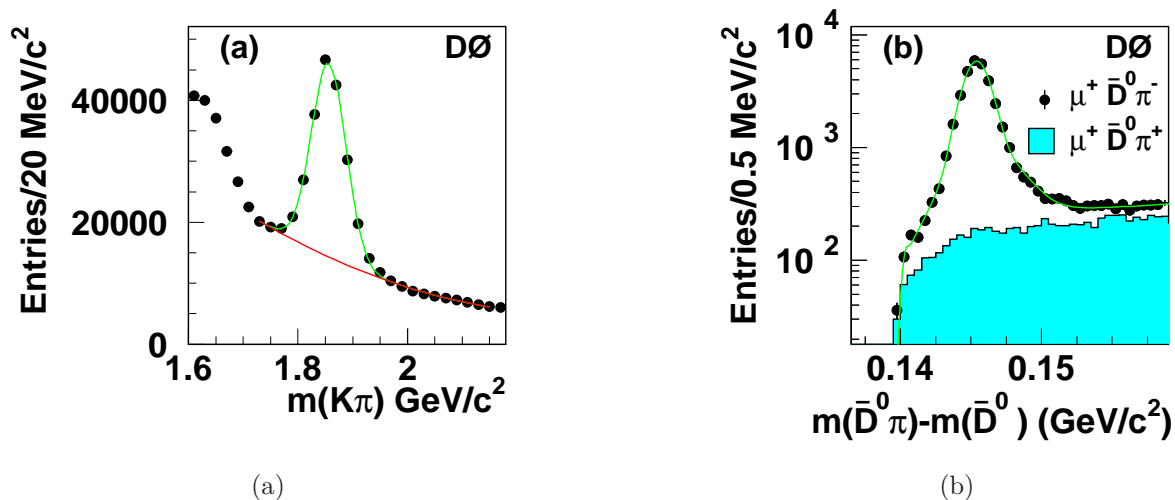


Figure 5: (a) Invariant mass of the $K\pi$ system. The curve shows the result of the fit of the $K^+\pi^-$ mass distribution. (b) Mass difference $\Delta m = m(\bar{D}^0\pi) - m(\bar{D}^0)$.

In Fig. 5, we show the invariant mass distributions for \bar{D}^0 and D^{*-} candidates, where they have been combined with a muon of the correct charge, *e.g.*, $B^+ \rightarrow \bar{D}^{(*)}\mu^+ X$. Fig. 5(b) also shows the wrong-sign spectrum; as expected there is no peak.

Candidate events are classified as D^0 and right (and wrong) sign D^* . From these categories, we determine the number of true $\bar{D}^0\mu^+$ and $D^{*-}\mu^+$ events in eight bins of visible proper decay length (VPDL), where $VPDL = m_{BC} \left(L_T \cdot p_T(\mu^+\bar{D}^0) \right) / |p_T(\mu^+\bar{D}^0)|^2$, and calculate the ratio, $r_i = \frac{N_i(D^{*-}\mu^+)}{N_i(\bar{D}^0\mu^+)}$. L_T is the transverse decay length of the $(\mu^+\bar{D}^0)$ vertex relative to the primary vertex, and p_T is the transverse momentum. To avoid any biases, for both \bar{D}^0 and D^{*-} samples, the soft pion is not used for determining VPDL or p_T .

Next we determine the expected ratio of events in each VPDL bin and minimize, $\chi^2 = \sum_i \frac{(r_i - r_i^e(\epsilon_\pi, k))^2}{\sigma^2(r_i)}$, where the lifetime ratio, $k = \tau^+/\tau^0 - 1$, and the efficiency of the slow pion ϵ_π are free parameters. The r_i^e 's are determined *ab initio* using B semi-leptonic branching fractions, detector resolution, a Monte Carlo simulation to account for missing particles, reconstruction efficiencies, and the world average for the B^+ lifetime; B^0 lifetime, τ^0 , is expressed as $\tau^0 = \tau^+/(1+k)$.

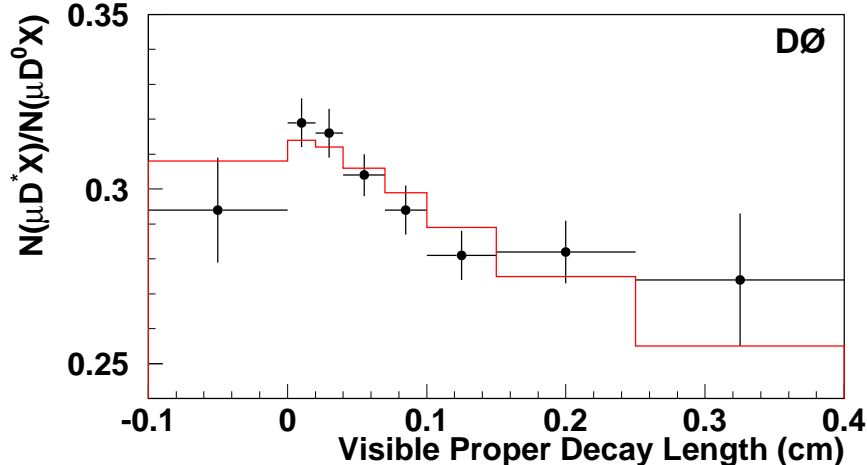


Figure 6: Points with the error bars show the ratio of the number of events in the μ^+D^{*-} and $\mu^+\bar{D}^0$ samples as a function of the visible proper decay length. The result of the minimization with $k = 0.080$ is shown as a histogram.

Minimization of the χ^2 distribution gives, $k = \tau^+/\tau^0 - 1 = 0.080 \pm 0.016(stat) \pm 0.014(syst)$. In Fig. 6, we show r_i as a function of VPDL; the fit results are overlaid. The systematic uncertainty includes uncertainties on B branching fractions, reconstruction efficiencies, detector resolutions, *etc.*

6.2 Measurement of $\tau(\Lambda_b)$

Theoretical predictions for the ratio, $\frac{\tau(\Lambda_b)}{\tau(B^0)}$ ($\sim (0.88 - 0.98)$ with errors $\sim \pm 0.02 - 0.05$)[26], have always been somewhat higher than experimental results[9], (0.80 ± 0.05) . One possible source for the discrepancy could be that all previous measurements used partially reconstructed Λ_b , which required one to use Monte Carlo simulations to correct for missing particles, *e.g.*, ν, π *etc.*. Since Λ_b decays have not been studied in detail, this correction process makes the result model dependent.

We measure $\tau(\Lambda_b)$, via the fully reconstructed decay, $J/\psi\Lambda$, with $J/\psi \rightarrow \mu^+\mu^-$, $\Lambda \rightarrow p\pi^-$, using $\sim 250 \text{ pb}^{-1}$ of integrated luminosity. For comparison, $\tau(B^0)$ is measured using the $J/\psi K_s^0$ mode ($K_s^0 \rightarrow \pi^+\pi^-$); the two modes have similar topology. We reconstruct 61 ± 12 and 291 ± 23 events, respectively[27].

In Fig. 7(a), we show the mass distribution of the Λ_b^0 candidate events, and in Fig. 7(b) their proper decay lengths are presented.

The lifetime was obtained by performing a unbinned likelihood fit using both the mass and the lifetime of candidate events. We used all events in the mass range $5.1\text{-}6.1 \text{ GeV}/c^2$ for Λ_b ($4.9\text{-}5.7 \text{ GeV}/c^2$ for B^0). Different functions were used to model the lifetime (and mass) of signal and background events.

We obtain, $\tau(\Lambda_b^0) = 1.22_{-0.18}^{+0.22} (stat) \pm 0.04 (syst) \text{ ps}$, and $\tau(B^0) = 1.40_{-0.10}^{+0.11} (stat) \pm 0.03 (syst) \text{ ps}$. This is the first time that the Λ_b lifetime has been measured in an exclusive channel; our result agrees with previous measurements[9]. We also obtain, $\frac{\tau(\Lambda_b^0)}{\tau(B^0)} = 0.87_{-0.14}^{+0.17} (stat) \pm 0.03 (syst)$. The current statistical error on the ratio is too large to draw any conclusions, however this error will decrease as more data is processed. The systematic uncertainty includes contributions from Silicon

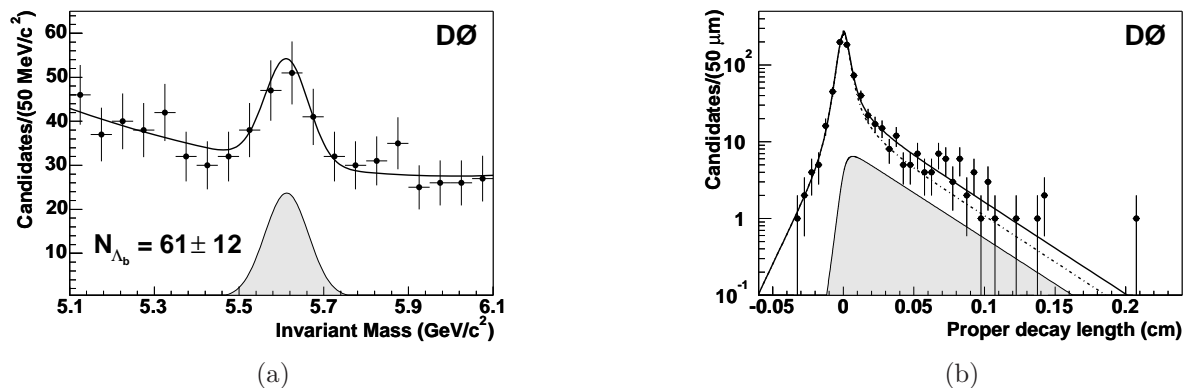


Figure 7: (a) Invariant mass distribution for Λ_b^0 candidate events. The points represent the data, and the curve represents the result of the fit. The mass distribution for the signal is shown in gray, (b) Distribution of proper decay length for Λ_b^0 candidates. The points are the data, and the solid curve is the sum of the contributions from signal (gray) and the background (dashed-dotted line)

alignment uncertainties, models used for signal and background and cross-feed between the $J/\psi\Lambda$ and $J/\psi K_s^0$ modes.

6.3 Measurement of $\tau(B_s^0)$

Theoretical calculations predict $\frac{\tau(B_s^0)}{\tau(B^0)} \sim 1.0 \pm \mathcal{O}(1\%)$ [23, 24]. The CP eigenstates of the $B_s^0 - \bar{B}_s^0$ system are expected to have different lifetimes[28]; predictions for $\frac{\Delta\Gamma_s}{\Gamma_s}$ are $\sim 10 - 20\%$. This difference can be probed by comparing the B_s lifetime measured using the semi-leptonic final state (which has equal mixtures of the two CP states) and using a decay like $J/\psi\phi$ (which is expected to be dominantly CP even). Alternatively, one could directly measure the lifetime difference using the $J/\psi\phi$ mode; this analysis has recently been performed by the CDF collaboration and they find $\frac{\Delta\Gamma_s}{\Gamma_s} = 65_{-33}^{+25} \pm 1\%$ [29].

Using $\sim 220 \text{ pb}^{-1}$ of integrated luminosity, DØ has measured the B_s^0 lifetime reconstructed in the $J/\psi\phi$ ($\phi \rightarrow K^+K^-$) final state[30]. In this analysis, we fit the B_s^0 lifetime with a single exponential, *i.e.*, under the assumption $\Delta\Gamma_s \sim 0$. For comparison, we also measure B^0 lifetime using the final state $J/\psi K^{*0}$ ($K^{*0} \rightarrow K^+\pi^-$), which has similar topology; the two modes have 337 and 1370 signal events, respectively.

In Fig. 8(a), we show the mass distribution of the B_s^0 candidate events, and in Fig. 8(b) their proper decay lengths are presented. The measurement technique is the same as the one used in the Λ_b lifetime analysis.

We find $\tau(B_s^0) = 1.444_{-0.090}^{+0.098} \text{ (stat)} \pm 0.020 \text{ (sys) ps}$, and $\tau(B^0) = 1.473_{-0.050}^{+0.052} \text{ (stat)} \pm 0.023 \text{ (sys) ps}$. Both results are consistent with world averages.⁶ In addition, we also measure, $\frac{\tau(B_s^0)}{\tau(B^0)} = 0.980_{-0.070}^{+0.075} \text{ (stat)} \pm 0.003 \text{ (syst)}$, which is in agreement with theoretical predictions.

⁶Since the B_s average ($1.461 \pm 0.057 \text{ ps}$)[9] is dominated by measurements made using semi-leptonic final states, our result appears to prefer a low value for $\frac{\Delta\Gamma_s}{\Gamma_s}$.

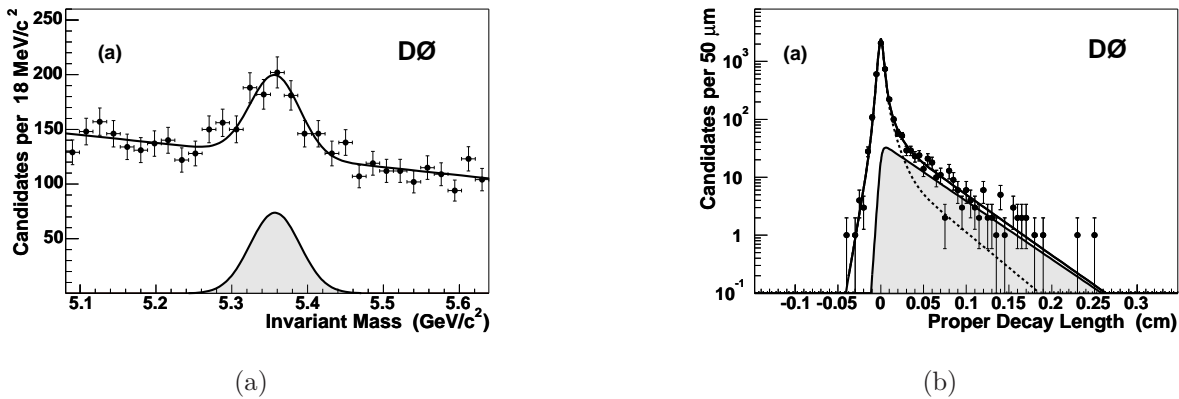


Figure 8: (a) Invariant mass distribution for B_s^0 candidate events. The points represent the data, and the curve represents the result of the fit. The mass distribution for the signal is shown in gray, (b) Distribution of proper decay length for B_s^0 candidates. The points are the data, and the solid curve is the sum of the contributions from signal (gray) and the background (dashed line)

7 $B_s\bar{B}_s$ Mixing

The phenomenon of particle-antiparticle mixing has yielded many unexpected results and has provided the impetus for significant progress in the field. For instance, the large rate of mixing in $B^0\bar{B}^0$ implied that the top quark was much heavier than previously expected and $K^0 - \bar{K}^0$ mixing taught us about CP violation. Quark mixing occurs at the one-loop level via “box” diagrams and heavy particles (in the loop) tend to have enormous influence[31].

The study of $B_s\bar{B}_s$ mixing has a twofold purpose. Given the previous successes of mixing induced processes, one could hope for a surprise. Failing an unexpected result, the measurement of the rate of $B_s\bar{B}_s$ mixing will aid in reducing the error on the measurement of the CKM element V_{td} [9]. If our current understanding of the Standard Model and the CKM matrix are correct[2], then B_s oscillations should occur with a frequency, ΔM_s , in the (95% CL) interval (14.2-28.1) ps^{-1} . A deviation could be a sign of new physics. Additionally, if the mixing parameter, ΔM_s is very large then the difference in the widths of the CP eigenstates of the B_s may be detectable.⁷

B oscillations are observed by comparing the proper time evolution of events where a neutral B-hadron decays as a particle of the opposite flavor from that with which it was produced (mixed B) to those where the B-hadron’s production and decay flavors are the same (unmixed B). To study B_s oscillations we therefore need three ingredients, (a) final state reconstruction, (b) ability to measure B decay lengths, and (c) flavour tagging of the B both at production and decay.

The significance of a B mixing measurement can be expressed as,

$$\text{Sig} = \sqrt{\frac{N\epsilon D^2}{2}} \exp^{-(\Delta M \times \sigma_t)^2/2} \sqrt{\frac{S}{S+B}} \quad (1)$$

where N is the number of reconstructed B_s events, ϵD^2 is a measure of how well we know the flavour of the B_s at production; ϵ is the efficiency of the tag, and D , the dilution is defined as $D = 1 - 2w$, where w is the probability of mis-identifying the flavour of the B-hadron at production. σ_t is the proper time resolution, and $S/(S+B)$ expresses signal purity. It is clear that as ΔM_s gets larger, the importance of good proper time resolution increases.

⁷This analysis is in progress.

At D0, B-mixing is studied mainly using semileptonic B^0 and B_s^0 decays, although a fully hadronic Bs decay mode analysis is in progress. The advantage of using semi-leptonic events vis-a-vis (fully reconstructed) hadronic events is that the branching fraction for the former is much larger than for the latter; the total rate for $B_s \rightarrow D_s \mu \nu + X$ is $\sim 10\%$, whereas the rate for $B_s \rightarrow D_s^{(*)-} \pi^+$ is $\sim 0.3\%$. The disadvantage of using semi-leptonic is that due to missing particles, the proper time resolution is worse.

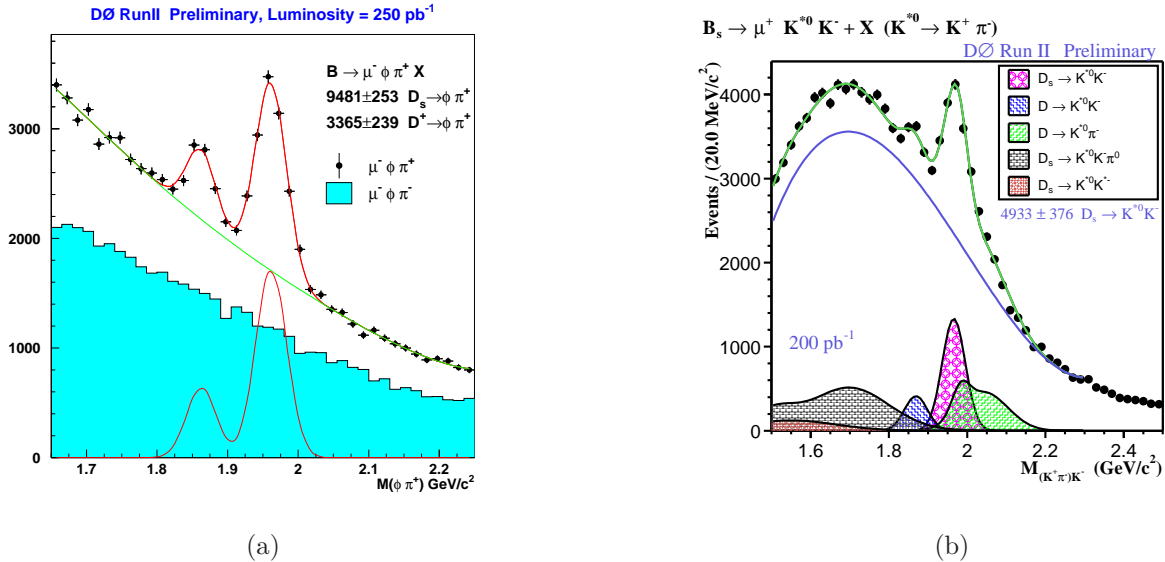


Figure 9: Invariant mass distribution for D_s^\pm candidate events where the D_s is charge correlated to the muon, such that the peaks correspond to right sign $B_s \rightarrow D_s \mu \nu + X$ events for (a) $D_s^+ \rightarrow \phi \pi^+$, (b) $D_s^- \rightarrow K^{*0} K^-$. The blue shaded histogram in (a) corresponds to wrong sign $D_s \mu$ combinations. The peaks in (b) correspond to D_s (D^+) signal and background.

In Fig. 9, we present the inclusive $B \rightarrow D_s \mu X$ signal for (a) $D_s^+ \rightarrow \phi \pi^+$ using 250 pb^{-1} and (b) $D_s^- \rightarrow K^{*0} K^-$ using 200 pb^{-1} . The peaks at the D_s mass are dominated by B_s decays.

The next component needed for a mixing measurement is knowledge of the flavour of the B hadron at the time of production and decay. By using flavour-specific decays, one can easily tag the flavour at the time of decay. To tag the B flavour at production we use the following techniques,

- **Soft Lepton Tagging:** The sign of the lepton produced in the semi-leptonic decay of the other B in the event is used to tag the flavour of the signal B . We then make the assumption that (at production) the flavour of the signal B is opposite to that of the tag B . This method has low efficiency, but very high tagging power. We are also using electrons, although those results are not final as yet.
- **Jet Charge Tagging:** We take all tracks opposite to the signal B and form a track jet, and measure its charge. The assumption is that these tracks are produced in the fragmentation of the other b-quark, as well as in the decay of the tag B hadron. This method has high efficiency, but has poorer tagging power.
- **Same Side Tagging:** In this technique, we identify particles produced in the fragmentation of the b-quark which gives rise to the signal B . In addition, the signal B can come from a resonance, *e.g.*, $B^{**+} \rightarrow B^0 \pi^+$, and the charge of such pions is correlated with the flavour

of the signal B at the time of production. This method has high efficiency, but has poorer tagging power.

We have tested our analysis by measuring the mixing parameter for $B^0\bar{B}^0$, *i.e.*, ΔM_d ; we use $\sim 200 \text{ pb}^{-1}$ for this study. In Fig. 10, we show the asymmetry as a function of visible proper decay length, where the asymmetry, $\mathcal{A}(t)$, is defined as $\frac{N_U - N_M}{N_U + N_M}$; $N_U(N_M)$ are the numbers of unmixed (mixed) events in the various time bins. In this analysis, we use the decay mode $B^0 \rightarrow D^{*-}\mu^+\nu + X$ events. In (a), we show the asymmetry for events tagged with a soft muon, whereas in (b) we show the asymmetry for events tagged with a combination of Jet Charge and Same Side taggers. A simultaneous fit to the two distributions in Fig. 10 yields $\Delta M_d = 0.456 \pm 0.034(\text{stat}) \pm 0.025(\text{syst})$, which is in agreement with the world average[9]. We also get the efficiency and dilution for the two tags to be, (a) $\epsilon = 5.0 \pm 0.2\%$ and $D = 44.8 \pm 5.1\%$, (b) $\epsilon = 68.3 \pm 0.9\%$ and $D = 14.9 \pm 1.5\%$, respectively.

Since ΔM_s is much larger than ΔM_d , it is clear from Eq. (1) that the critical element is the proper time resolution. Work is underway to improve the resolution for semi-leptonic final states.

We also have other improvements in the pipeline that will have significant impact on the ΔM_s analysis: (a) A new layer of silicon sensors will be installed at a radius of 2.5 cm. This is expected to improve the proper time resolution by about 25%, (b) An increase in the trigger bandwidth will enable us to increase the yield of “B-rich” events many-fold, and (c) Improved triggers will enrich the data with hadronic B_s decays.

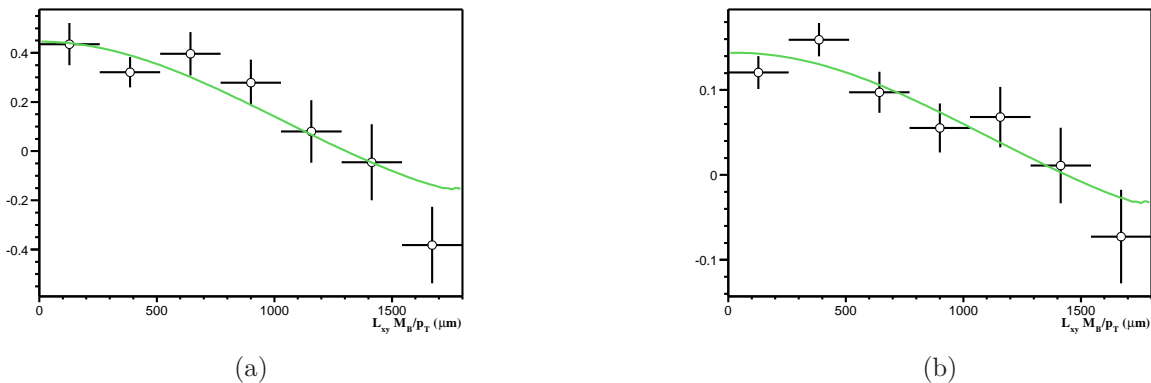


Figure 10: Asymmetry distributions for $B^0 \rightarrow D^{*-}\mu^+\nu + X$ events, using (a) the soft muon tag, (b) a combination of jet charge and same side tags.

8 Conclusions

The D0 detector has started to produce very competitive results in the field of B physics. We have already recorded $\sim 520 \text{ pb}^{-1}$ of data and hope to collect $\sim 1 \text{ fb}^{-1}$ by the end of 2005 and $\sim 4(8) \text{ fb}^{-1}$ by the end of 2007 (2009).

As a stepping stone to B_s mixing, we have measured ΔM_d to benchmark our analyses techniques. In addition, we are pursuing a vigorous program which includes measurement of B lifetimes, rare decays, studies of quarkonia[32], beauty baryons and B_c .

Acknowledgments

I would like to thank Hal Evans, Brad Abbott and Jesse Ernst for stimulating discussions.

References

- [1] Excellent reviews of B physics can be found in (a) BaBar Physics Handbook at <http://www.slac.stanford.edu/pubs/slacreports/slac-r-504.html>; (b) B Physics at the Tevatron: Run II and beyond, <http://xxx.lanl.gov/~hep-ph/0201071>; (c) A.G. Akeroyd *et al.*, “Physics at Super B factory”, <http://xxx.lanl.gov/~hep-ex/0406071> and in references therein.
- [2] M. Battaglia, *et al.*, “The CKM matrix and the unitarity triangle”, Tech. rep., hep-ph/0304132 (2003).
- [3] Private communication with Ulrich Nierste.
- [4] V. Abazov, *et al.*, DØ Collab., “The Upgraded DØ Detector”, in preparation for submission to Nucl. Instrum. Meth. Phys. Res. A; T. LeCompte and H.T. Diehl, “The CDF and DØ upgrades for Run II”, Ann. Rev. Nucl. Part. Sci. **50**, 71 (2000).
- [5] http://www-d0.fnal.gov/Run2Physics/ckm/Approved_results/index2.html
- [6] Belle Collaboration, S.K. Choi *et al.*, Phys. Rev. Lett. **91**, 262001 (2003); CDF Collaboration, D. Acosta *et al.*, Phys. Rev. Lett. **93** 072001 (2004)
- [7] DØ Collaboration, V.M. Abazov *et al.*, Phys. Rev. Lett. **93** 162002 (2004)
- [8] E. J. Eichten, K. Lane and C. Quigg, Phys. Rev. **D 69**, 094019 (2004) and references therein.
- [9] S. Eidelman *et al.*, Phys. Lett **B 592**, 1 (2004)
- [10] A recent review can be found in N. Isgur, Phys. Rev. **D 57**, 4041 (1998). More details can be found in the references therein.
- [11] Belle Collaboration, K. Abe *et al.*, Phys. Rev. **D 69**, 112002 (2004)
- [12] BaBar Collaboration, B. Aubert *et al.*, Phys. Rev. Lett **90**, 242001 (2003); CLEO Collaboration, D. Besson *et al.*, Phys. Rev. **D68**, 032002 (2003)
- [13] For instance, see E. Eichten’s talk at the 6th International Conference on Hyperons, Charm and Bottom Hadrons, Illinois Institute of Technology, Chicago, USA, June 27-July 3, 2004.
- [14] For instance, see predictions in E.J. Eichten, C.T. Hill and C. Quigg, Phys. Rev. Lett. **71**, 4116 (1993)
- [15] Recent reviews can be found in D. Ebert *et al.*, Phys. Rev **D 68**, 094020 (2003); M. Beneke, *et al.*, Phys. Rev. **D 53**, 4991 (1996); I.I. Bigi Nucl. Instrum. Meth. **A 351** 240-247 (1994) and in references therein.
- [16] CDF Collaboration, F. Abe *et al.*, Phys. Rev. **D 58**, 112004 (1998).
- [17] D. Scora *et al.*, Phys. Rev. **D 52**, 2783 (1995)

- [18] D0 Collaboration, D0Note 4539-CONF, Aug. 16, 2004. Available at <http://www-d0.fnal.gov/Run2Physics/WWW/results/prelim/B/B12/B12.pdf>
- [19] A.J. Buras, Phys. Lett. **B 566**, 115 (2003)
- [20] CDF Collaboration, D. Acosta *et al.*, Phys. Rev. Lett. **93**, 032001 (2004)
- [21] Please see references [5]-[11] in V.M. Abazov *et al.*, FERMILAB-Pub-04/215-E, hep-ex/0410039 (2004)
- [22] DØ Collaboration, V.M. Abazov *et al.*, FERMILAB-Pub-04/215-E (hep-ex/0410039). Accepted in Phys. Rev. Lett.
- [23] N. Uraltsev, in *At the Frontier of Particle Physics: Handbook of QCD*, edited by M. Shifman (World Scientific, Singapore, 2001), hep-ph/0010328 (2001); G. Bellini, I.I. Bigi, P.J. Dornan, Phys. Rep. **289**, 1 (1997)
- [24] C. Tarantino *et al.*, Eur. Phys. J. **C33** (2004) S895-S899, hep-ph/0310241 (2003); Other estimates can be found in Gabbiani *et al.*, Phys. Rev. **D70**, 094031 (2004)
- [25] DØ Collaboration, V.M. Abazov *et al.*, FERMILAB-Pub-04/284-E (hep-ex/0410052). Submitted to Phys. Rev. Lett.
- [26] Please see references [3], [5] and [6] in V.M. Abazov *et al.*, Phys. Rev. Lett. **94**, 102001 (2005); P. Colangelo and F. De Fazio, Phys. Lett. B **387**, 371 (1996)
- [27] V.M. Abazov *et al.*, Phys. Rev. Lett. **94**, 102001(2005)
- [28] I. Bigi *et al.* in “B Decays”, 2nd edition, edited by S. Stone (World Scientific, Singapore 1994) p. 13 ; I. Dunietz, Phys. Rev. D **52**, 3048 (1995); M. Beneke, G. Buchalla, I. Dunietz, Phys. Rev. D **54**, 4419 (1996)
- [29] CDF Collaboration, D. Acosta *et al.*, hep-ex/0412057
- [30] V.M. Abazov *et al.*, Phys. Rev. Lett. **94** 042001, (2005)
- [31] See A. J. Buras and R. Fleischer, hep-ph/9704376 for a comprehensive exposition of quark mixing and other related topics
- [32] D0 Collaboration, D0Note 4523-CONF, Aug. 2, 2004. Submitted to Phys. Rev. Lett. Available at <http://www-d0.fnal.gov/Run2Physics/WWW/results/prelim/B/B09/B09.pdf>; A comprehensive review of latest theory and experimental results on Quarkonia can be found in the CERN Yellow report by the Quarkonium Working Group - hep-ph/0412158